Meteorol. Z. (Contrib. Atm. Sci.), Vol. **31**, No. 2, 117–130 (published online February 4, 2022)

A wind atlas for Germany and the effect of remodeling

Martin Schneider[1*], André Glücksmann[1], Anselm Grötzner[2] and Heinz-Theo Mengelkamp[1]

[1]anemos Gesellschaft für Umweltmeteorologie mbH, Reppenstedt, Germany
[2]Ramboll Deutschland GmbH, Kassel, Germany

(Manuscript received June 28, 2021; in revised form November 19, 2021; accepted November 23, 2021)

Abstract

Minimizing and quantifying the uncertainty of wind simulations are essential for the wind energy industry during the planning phase of wind farm projects and for financial considerations. Measurements at 118 sites onshore and offshore in Germany are analyzed and used for the verification of wind simulations with the mesoscale model WRF. In order to minimize the difference between simulations and observations a correction of the annual cycle is applied and a remodeling approach is developed which allows for a correction of the simulated wind speed time series. The remodeling methodology is based on a linear regression analysis of simulated and observed wind speed time series accounting for sub-grid variations of orography and roughness. Averaging the regression parameter for 26 measurement sites results in an overall global parameter set which is applied to the wind atlas data. While the "raw" data (without optimization) before any correction showed differences of up to 30 % with respect to the annual mean wind speed the remodeling process reduced the bias to below 5 % for the majority of measurements. When being compared with data from the NEWA wind atlas and the EMD-WRF Europe+ data set an overall bias between 0.6 m/s and 0.8 m/s is found for the NEWA, EMD-WRF Europe+ and anemos "raw" data. This bias is reduced to zero with a small standard deviation when the remodeling process and the site-specific adaptation are applied.

Keywords: mesoscale model verification, wind atlas, wind measurements, adaptation of wind simulations

1 Introduction

The wind energy industry has developed dramatically during the last three decades and wind power now has a major share in the transformation from fossil fuels to renewable energy. Parallel to this trend wind power meteorology has evolved with focus on three main areas, namely the short-term prediction of electricity production, site suitability (turbulence and extreme winds in order to estimate the mechanical stress on wind turbines) and resource assessment. Reducing the uncertainty in wind speed and direction simulations is of utmost importance for wind farm developers, investors and financing institutions. Even small errors can have a large impact on financial considerations as the electricity production by wind turbines increases non-linearly with respect to wind speed. Therefore, it remains a major challenge for the wind power meteorological community to minimize the uncertainty in wind resource assessment to the extent possible. This study focuses on resource assessment on regional to local scales and the quantification of its uncertainty through the comparison of model simulations with observations.

Since its early stages wind resource assessment has been based on statistical methods (Petersen et al., 1981; Mengelkamp, 1999; Mengelkamp et al., 1997; Badger et al., 2014). Estimating the site-specific wind potential in terms of the wind speed frequency distribution has been the preferred approach for energy yield calculations (Serban et al., 2020) and is still widely applied today. However, approximating the energy of the wind by statistical means is never totally perfect compared to time series. Moreover, wind turbines have to be shut down temporally i.e. for noise reduction or bat protection during nighttime and time series analysis is required to accurately estimate the yield losses. When information is needed of the market value of the electricity produced a temporal correlation with the variable stock exchange price for electricity is essential. Highly accurate site-specific time series of the energy yield are appropriate means to meet the requirements for sound financial considerations during the wind farm planning phase. As the life time of wind turbines is assumed more than 20 years the time series should span a climatologically relevant time period of a similar length.

Reliable wind information over two or more decades is rarely available from observations. Except a few towers for research purposes the majority of observations of wind speed and wind direction takes place near the surface and is influenced by surface characteristics (orography, roughness, obstacles) in the immediate surrounding (Wieringa, 1980, 1996). Weather station data seem to be the first choice but Lindenberg et al. (2012) have shown that such data are inconsistent in time due to changes in the instrument location or due to changes in surface characteristics of the surrounding area. In addition, near surface measurements do not reflect the wind conditions (i.e. the diurnal cycle, low level jets) in heights over 100 m which is exceeded by modern wind turbine hub heights. Site-specific wind measurements

*Corresponding author: Martin Schneider, anemos GmbH, Böhmsholzer Weg 3, 21391 Reppenstedt, Germany, e-mail: martin.schneider@anemos.de

during the planning phase of a wind farm commonly only span a short time period of usually 12 months and require a long-term correlation with a consistent long-term wind data set. In addition, hub heights of modern wind turbines will often reach more than 150 m. Measurements at these heights are cost intensive and are often aimed to be avoided.

Downscaling reanalysis data by use of a mesoscale model seems an appropriate approach to derive regional or local scale wind information. Motivated by the importance of mesoscale model simulations for the wind industry the Weather Research and Forecast mesoscale model WRF (WRF, 2017; Skamarock et al., 2008) has become a major tool for investigations into wind conditions and sensitivity studies. The latter mainly examine the influence of different PBL schemes (Fernández–Gonzales et al., 2018, Yang et al., 2013), or a combination of PBL schemes, grid configuration and initial conditions (Siuta et al., 2017). Carvalho et al. (2014) applied different reanalysis data sets to drive the mesoscale model WRF and compared the simulated hourly time series of wind speed and -direction with observations. An overall positive wind speed bias is explained by the smoothing of orography in the model caused by its limited spatial resolution. There was no best model configuration for all conditions and an ensemble of model runs is often suggested (Fernández-Gonzales et al. 2018, Siuta et al., 2017, Deppe et al., 2013) together with some kind of bias correction when using model simulations for "real world" applications such as financial considerations (Siuta et al., 2017, Deppe et al., 2013).

Weiter et al. (2019) follow the idea of using the electricity production from wind turbines directly for the verification of wind simulations. They transferred wind speed time series from simulations with the WRF model to production by use of the respective wind turbine power curves. The production data from operational wind turbines were analyzed very carefully in order to reflect the wind conditions without any influence of the wake effects and operation mode of the turbines. For 10-min data from 50 turbines in 12 windfarms the relative bias in production ranges between 10 % and 25 % which in terms of wind speed means a bias of 4 % to 10 % for the annual mean. This seems to be an acceptable uncertainty for financial considerations in the wind industry. In order to reach such small uncertainty numbers a bias correction was applied to the wind speed time series.

This paper aims at optimizing a wind atlas for Germany by a remodeling process and verifying the optimized wind speed time series. It is organized as follows. Details of the wind atlas simulation are given in the next section. The observational data used for the adaptation and verification are described in Section 3 and the remodeling approach and its expansion compared to the approach described in Weiter et al. (2019) in Section 4. Section 5 presents the comparison of model simulations with observations. There are two further wind data sets almost identical to the one described in this paper. The New European Wind Atlas (Gottschall et al., 2019; Witha et al., 2019; González-Rouco et al., 2019; Dörenkämper et al., 2020) and the EMD-WRF Europe+ (ERA5) mesoscale data set (EMD, 2020a, b) both were simulated with the mesoscale model WRF with 3 km horizontal resolution based on ERA5 reanalysis data. These two data sets cover all of Europe and are described and compared to our data set with the same forcing data and the same horizontal resolution for the WRF mesoscale model for Germany in Section 5.4. Section 6 comprises a summary and a brief outlook.

2 Model set-up and wind atlas simulation

The mesoscale model WRF (Weather Research & Forecasting Model version 3.7.1) (Skamarock et al., 2008; WRF, 2017) is used to downscale ERA5 reanalysis data (C3S, 2017) to the region of Germany (Fig. 1). A two-way nesting approach is realized to downscale the ERA5 reanalysis data with a horizontal resolution of approx. $30 \times 30\,\mathrm{km}^2$ to two domains with $9 \times 9\,\mathrm{km}^2$ for the outer domain and $3 \times 3\,\mathrm{km}^2$ for the inner nested domain, respectively. 50 vertical levels are prescribed up to the upper boundary at roughly 15 km height with 14 levels in the lowest 300 m which are most relevant for wind energy applications. Initial and boundary conditions were taken from the ERA5 data which are nudged (grid nudging method) into the WRF model every hour. The specific and the relaxation zone (the first five rows and columns in each domain) have boundary conditions from the reanalysis or values blended from the coarser domain, respectively. The WRF User Guide provides more information on the model operation.

Model output is stored every 10 minutes for a transient simulation starting in 1997 and still continuing. Thus, more than 24 years simulation are currently available. Different long-year simulations were distributed on several CPU with a one-month spin-up time each.

Orography data are taken from the SRTM (Shuttle Radar Topography Mission, USGS EROS Data Center, Farr et al., 2007) and interpolated from its 90 m resolution onto the model grid. Vegetation and roughness information is provided by the CORINE data (Keil et al., 2010) of the European Environment Agency and is interpolated from its 100 m resolution. Soil temperature and soil moisture at 4 soil levels and snow cover are taken from the ERA5 data set (C3S, 2017).

The WRF model contains many different schemes for the parameterization of physical processes. WRF's physics parameterization considered here is the Yonsei University (YSU) planetary boundary layer scheme, the Monin-Obukhov surface layer description, the Noah land surface model including Mosaic 4, the RRTM scheme for the longwave radiation, and the Dudhia parameterization for the short-wave radiation. No cumulus parameterization is applied (Skamarock et al., 2008).

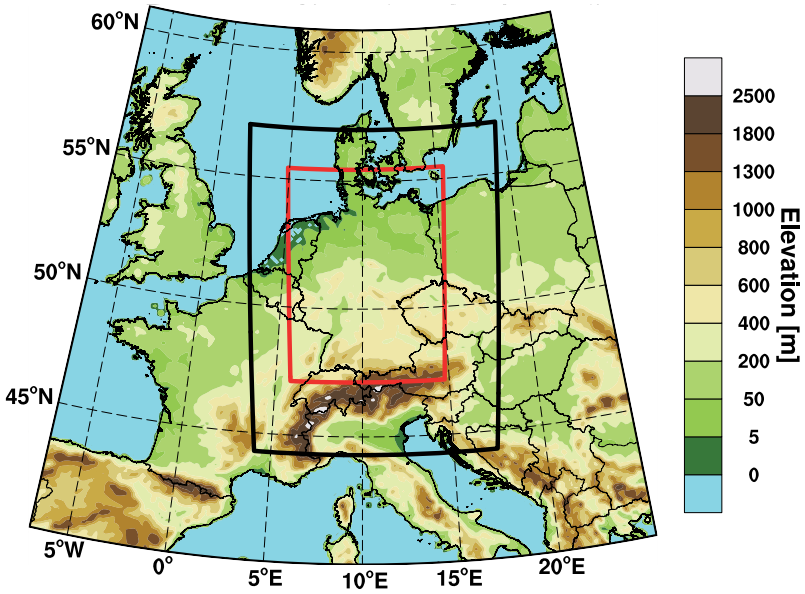

Figure 1: WRF model domain over Germany. Multiple Nesting with domain 1 ($9 \times 9\,\mathrm{km}^2$) and domain 2 ($3 \times 3\,\mathrm{km}^2$).

Despite the many sensitivity studies mentioned the one optimal set-up for wind energy applications hardly exists. A model performing best in a certain situation over a certain region may not do so at other circumstances. In several of the studies cited ensemble simulations were suggested to be most appropriate. However, limited resources did not allow us to perform ensemble simulations nor to undertake extensive sensitivity studies as done by Olsen et al. (2017) and Hahmann et al. (2020). Also, ensemble and sensitivity studies reflect the behavior of different model set-ups rather than the uncertainty with respect to observations which only is relevant for wind energy applications. As the near surface winds are most sensitive to the choice of the PBL scheme (Hahmann et al., 2020) an investigation into the most appropriate PBL scheme for wind simulations has been undertaken comparing the wind conditions above 100 m height at 10 sites as simulated with the YSU and MYJ PBL schemes for August and December 2012. These schemes are widely applied in WRF simulations and seem to be appropriate for wind simulations in the boundary layer (Hu et al., 2010, 2013), A best scheme for all situations and sites cannot be proposed (Giannakopoulou et al., 2014). The YSU scheme performed reasonably when wind speed profiles and the diurnal cycle were compared to measurements at our 10 sites.

3 Observational data

It is with the growing wind industry during the last two decades that a reasonable number of meteorological towers has been installed with heights of more than 100 m meanwhile. These towers usually are operated only for a period of one year and are privately owned. Given access to their data they form an excellent data base for model verification. This also holds for lidar measurements which, with increasing wind turbine hub height, become more advantageous by reason of financial and permit issues. A few research towers are operated by public institutions onshore and offshore within the model domain for periods of several years. In this study we used data from onshore and offshore research towers and short term measurements for wind farm planning purposes at met masts and with lidar devices. The observational uncertainty is considered very low as all towers and lidar measurements were erected for wind energy planning purposes and followed international recommendations (IEC, 2017) or were installed as research towers. Calibration sheets for all anemometers of the wind energy towers and for all lidar systems were available. The instrumentation of the research towers is considered to be maintained on a regular basis. All data were measured as 10-min averages and aggregated to hourly values for the verification while the remodeling approach is based on the 10-min measurements.

Two data sets are used for this study. Data set 1 comprises data from 48 onshore met masts and lidars of which 26 are used for the remodeling process and 22 for the independent verification. Measurements at the four offshore masts FINO1 (North Sea), FINO2 (Baltic), FINO3 (North Sea), and NordseeOst (North Sea) are used for the verification and separate offshore remodeling. All these data are at the hands of anemos. In order to support the verification results with a second independent data set wind speed time series of the wind atlas simulation were provided to the consulting company Ramboll for 66 locations at which they had tall mast and lidar measurements available from their consulting activities. It is ensured that those data are of similar very high quality as the first data set and that they are analyzed in a similar way. The analysis of the measurements covers a plausibility check, identification of icing periods and missing values for any reason and a

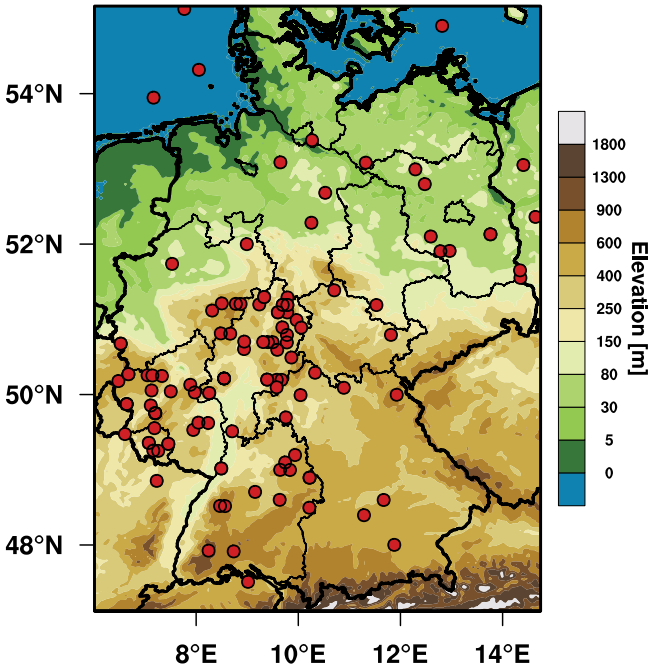

Figure 2: Geographical distribution of measurement sites.

correction for mast shadow effects in case of only one anemometer per height was installed. If two anemometers were installed at the respective height pointing into opposite directions the undisturbed data were used. A correlation among all wind measurements at the same mast helped to identify any implausible data. In summer 2009 east of FINO1 the offshore wind farm "alpha ventus" was erected with influence on the FINO1 measurements for easterly winds. Only FINO1 data before this date are used in this study. Similarly, if disturbances occurred during the measuring period e.g. due to extension of a wind farm, this particular met mast was excluded from this study or data from times before the disturbance affected them were used only. For each measurement station a 12-month period was selected, but not necessarily the same period for all stations, because the simulation covers more than 24 years. All measurement stations should reach data availability of at least 80 %. Periods of missing observations were also eliminated from the respective simulated time series. The measurements were distributed all over Germany with the majority of them in complex terrain in the southwestern parts, two in the western part of Poland and one in the northern part of Switzerland. (Fig. 2).

4 Verification and remodeling

We denote the wind speed at different stages of the remodeling process as follows.

$u_{\mathrm{WRF}}^{\mathrm{cell\ raw}}$ is the raw wind speed as simulated in the model grid cell center without any adaptation.

$u_{\mathrm{WRF}}^{\mathrm{site\ raw}}$ is the raw wind speed before the remodeling process but made comparable to the site of a wind measurement according to step 2.

$u_{\mathrm{WRF}}^{\mathrm{cell\ rem}}$ is the wind speed at the grid cell center after the remodeling described in step 3.

$u_{\mathrm{WRF}}^{\mathrm{site\ rem}}$ is the wind speed after the remodeling process made comparable to wind measurement sites following step 4 resp. step 2.

A verification is performed twice, before and after the remodeling process in order to demonstrate the effect of the remodeling on the wind atlas. For both, the verification and the remodeling process observations and model simulations have to be made comparable. While the model grid cell height is an average for the $3 \times 3\,\mathrm{km}^2$ area a met mast for wind energy purposes commonly is placed at an exposed location advantageous for wind farm operation. An elevation and roughness correction for wind speed is applied on the model data that accounts for speed-up effects over unresolved crests (Howard and Clark, 2007). This correction has been developed with the computational fluid dynamics (CFD) code Meteodyn WT (2015). The difference between the site-specific wind speed and the wind speed at the 3 km grid cells was compared at 10 sites to the height difference $\Delta h = h_{\mathrm{site}} - h_{\mathrm{cell}}$ and the roughness difference $\Delta z_0 = z_{0\mathrm{site}} - z_{0\mathrm{cell}}$. It results in the empirically derived speed-up factors α and β. This correction accounts for the height difference Δh between the elevation asl of a particular measurement site and the elevation of the model grid cell and the difference Δz_0 in roughness length. Because the roughness tables for Meteodyn and WRF differ but are both based on the Corine data set, the roughness table from WRF was transferred into the roughness table for Meteodyn. The correction changes the original model wind speed output $u_{\mathrm{WRF}}^{\mathrm{cell\ raw}}$ to the wind speed $u_{\mathrm{WRF}}^{\mathrm{site\ raw}}$ adapted at the site of the measurements but still with systematic errors of the simulation. This step only makes the simulated data comparable to the measurements at a particular site

$$u_{\mathrm{WRF}}^{\mathrm{site\ raw}} = u_{\mathrm{WRF}}^{\mathrm{cell\ raw}} \cdot (1 + \Delta h \cdot \alpha + \Delta z_0 \cdot \beta) \qquad (4.1)$$

with α and β being constants in units of m^{-1} empirically derived at 10 sites different from the ones used in this study. α and β were developed from speed-up factors found by CFD model simulations at the respective 10 sites.

4.1 Remodeling

An optimization approach is applied to the wind speed time series of the lowest levels up to 300 m of the site-adapted raw WRF simulation $u_{\mathrm{WRF}}^{\mathrm{site\ raw}}$.

The remodeling process is based on a comparison of simulated wind speed time series $u_{\mathrm{WRF}}^{\mathrm{site\ raw}}$ with observations at 26 met masts onshore in a height range of 80 to 140 m. A separate correction function was derived for the offshore met masts. Because there were only 4 offshore masts no independent data were available for the verification.

The remodeling or optimization of the simulated wind speed $u_{\mathrm{WRF}}^{\mathrm{cell\ raw}}$ basically consists of four steps:

1. The first step is a correction of the annual cycle of the "raw" wind speed data of the WRF simulation on the $3 \times 3\,\mathrm{km}^2$ grid ($u_{\mathrm{WRF}}^{\mathrm{cell\ raw}}$). Since ERA5 reanalysis data and consequently the raw data of the wind atlas from the WRF simulation driven by ERA5 show a bias of the annual cycle, a correction of this was implemented in the optimization approach. The monthly bias of 48 onshore stations was analyzed. The mean bias of each month is used to determine a correction function for the annual cycle. Finally, a periodic function with amplitude and phase derived from the mean bias values generates time dependent and periodic scaling factors for each 10-min time step. This scaling factor time series is multiplied with the wind speed time series. This approach successfully minimized the monthly bias and did not impair other statistical parameters. The annual cycle correction is based on the bias of all 48 onshore met masts while the following remodeling steps use only 26 data sets for training. A separate annual cycle correction was derived for the offshore locations.

2. At this stage the simulated wind speed time series on the $3 \times 3\,\mathrm{km}^2$ grid $u_{\mathrm{WRF}}^{\mathrm{cell\ raw}}$ are made comparable to the observations with a correction based on elevation and roughness according to equation (4.1) resulting in $u_{\mathrm{WRF}}^{\mathrm{site\ raw}}$.

3. In a third step, both modeled $u_{\mathrm{WRF}}^{\mathrm{site\ raw}}$ and observed u_{obs} wind speed data with 10-min resolution are partitioned into eight wind direction sectors to account for various surface characteristics depending on wind direction sector δ. A linear regression analysis

$$u_{\mathrm{obs}}(\delta) = m(\delta) \cdot u_{\mathrm{WRF}}^{\mathrm{site\ raw}} + b(\delta) \tag{4.2}$$

follows for simulated and observed wind speed providing regression coefficients for each measurement site and 8 wind direction sectors, respectively.

There are now 16 regression coefficients for each of the 26 measurement sites (offset and slope of the regression line for each of 8 wind direction sectors). Following Staffell and Pfenninger (2016) and Thøgersen et al. (2007) a multiple linear regression analysis is performed separately for slope and offset parameter taking into account sub-grid information. The sub-grid information is taken from the respective variables on a $1 \times 1\,\mathrm{km}^2$ grid within each $3 \times 3\,\mathrm{km}^2$ cell for the height (x_1), the height difference between the respective $1 \times 1\,\mathrm{km}^2$ grid and $3 \times 3\,\mathrm{km}^2$ cell (x_2), the latitude (x_3) and the surface roughness (x_4). For each of the 26 sites (i) and for each of 8 direction sectors (j) this results in the equation for m

$$m_{i,j} = c_{0i,j} + c_{1i,j} \cdot x_{1i,j} + c_{2i,j} \cdot x_{2i,j} + c_{3i,j} \cdot x_{3i,j} + c_{4i,j} \cdot x_{4i,j} \tag{4.3}$$

and for $b_{i,j}$ accordingly. A multiple linear regression is applied on these sets of equations resulting in a set of global slope and offset parameter c_0 to c_4

$$m' = c_0 + c_1 \cdot x_1 + c_2 \cdot x_2 + c_3 \cdot x_3 + c_4 \cdot x_4 \tag{4.4}$$

and similarly for b'. The goal of this step is the calculation of global slope- and offset-parameter ($c_{0\text{–}4}$) for the investigated type of sub-grid information ($x_{1\text{–}4}$) from the training data. Finally, the c_1 till c_4 parameters are in a range between zero and one.

With the global scaling parameter derived from the 26 training met masts scaling factors are applied for the wind speed at each model grid cell taking into account the respective sub-grid information. The scaling factors are applied for each wind direction sector and result in a corrected simulated wind data set $u_{\mathrm{WRF}}^{\mathrm{cell\ rem}}$ for the $3 \times 3\,\mathrm{km}^2$ grid cells.

4. Site-specific time series $u_{\mathrm{WRF}}^{\mathrm{site\ rem}}$ are calculated from the $3 \times 3\,\mathrm{km}^2$ data $u_{\mathrm{WRF}}^{\mathrm{cell\ rem}}$ by applying step (2) again but now on the remodeled data.

The remodeling process changed the wind speed frequency distribution and the vertical wind speed profile at some sites in a non-acceptable way. Constraints for the frequency distribution were applied in the remodeling approach to minimize the error. A 0.1 % bias threshold was implemented for both tails of the frequency distribution, so that the $m_{i,j}$ and $b_{i,j}$ were slightly rescaled in the remodeling process until this threshold has reached. The analysis of different heights in the remodeling approach resulted in a vertical correction of the global parameters to reduce the bias at most of the heights. This vertical correction is handled by a height dependent scaling factor derived as a mean from the training set. The raw and corrected vertical profiles for station 19 are shown in Fig. 4 exemplary and the wind speed frequency distribution in Fig. 5.

The results of the remodeling process were verified with data from 48 onshore met masts. The raw data $u_{\mathrm{WRF}}^{\mathrm{cell\ raw}}$ show a clear positive bias of 0.7 m/s while a slight overcorrection of the remodeling on the $3 \times 3\,\mathrm{km}^2$ grid ($u_{\mathrm{WRF}}^{\mathrm{cell\ rem}}$) results in a negative bias of −0.4 m/s. Site-specific time series $u_{\mathrm{WRF}}^{\mathrm{site\ rem}}$ show no mean bias and also the lowest bias variation (Fig. 6).

4.2 Verification metrics

The primary objective of the wind atlas is its use for wind energy purposes. This basically requires frequency distributions of wind speed and -direction to characterize the local or areal wind climate. Additional information is provided by time series which reflect the temporal variability of the wind speed.

The mean wind speed is denoted as $\bar{u}$ and calculated as

$$\bar{u} = \frac{1}{n} \sum_{i=1}^{n} u_i \tag{4.5}$$

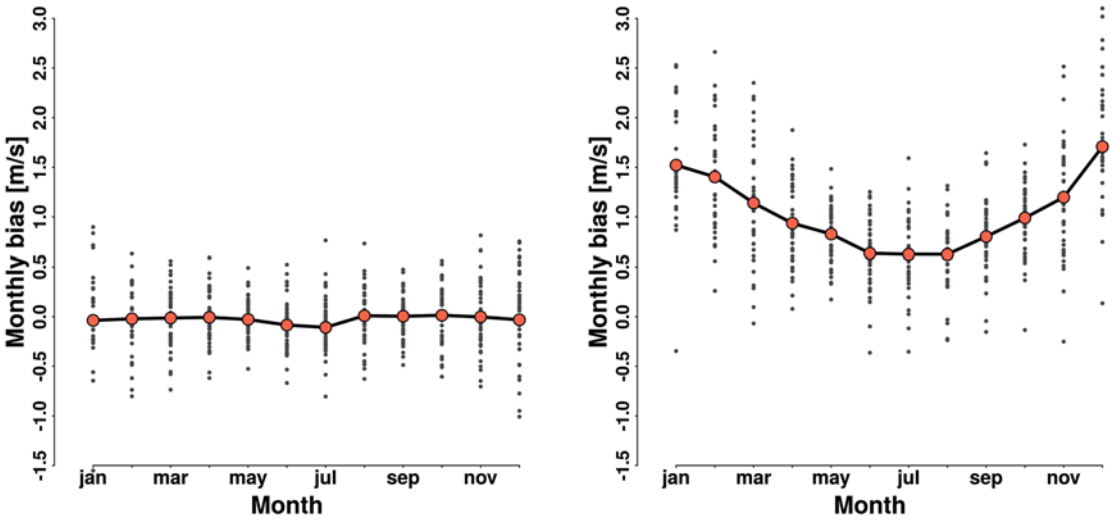

Figure 3: Bias in simulated monthly mean wind speed at 48 measurement locations. Right: Raw data, Left: after correction (line: mean bias, dots: individual measurements)

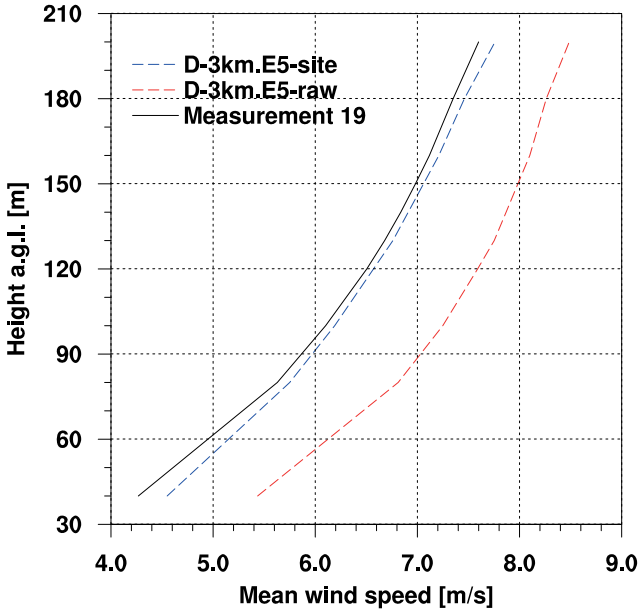

Figure 4: Exemplary vertical profiles of wind speed before (red) and after (blue) the remodeling process for measurement site 19.

with n being the total number of hourly data. The Pearson correlation coefficient R

$$R = \frac{\sum_{i=1}^{n}(u_{\mathrm{obs}_i} - \bar{u}_{\mathrm{obs}})(u_{\mathrm{WRF}_i} - \bar{u}_{\mathrm{WRF}})}{\sigma_{u_{\mathrm{obs}}}\sigma_{u_{\mathrm{WRF}}}} \tag{4.6}$$

is a measure for the temporal interrelation between measured "obs" and simulated "WRF" data.

The bias as the difference between mean values $\bar{u}_{\mathrm{WRF}} - \bar{u}_{\mathrm{obs}}$ or their ratio $\bar{u}_{\mathrm{WRF}}/\bar{u}_{\mathrm{obs}}$ points out a systematic deviation.

$$\mathrm{Bias}_{\bar{u}} = \bar{u}_{\mathrm{WRF}} - \bar{u}_{\mathrm{obs}} \tag{4.7}$$

And the mean bias is:

$$\overline{\mathrm{Bias}} = \frac{1}{m}\sum_{j=1}^{m}\mathrm{Bias}_j \tag{4.8}$$

with m being the number of verification sites. The standard deviation of the bias is

$$\sigma_{\mathrm{Bias}} = \sqrt{\frac{1}{m}\sum_{j=1}^{m}(\mathrm{Bias}_j - \overline{\mathrm{Bias}})^2} \tag{4.9}$$

Model data are instantaneous data every 10 minutes and observations are averages over a 10-min time interval. The remodeling procedure is based on these 10-min data while the verification is based on 1 h averages which should minimize the differences and is considered adequate for the verification of the diurnal cycle. A small shift in timing of changes in wind speed may lead to lower correlations, which, however, are insignificant for wind energy planning purposes (This paper does not cover short-term forecasts).

5 Results

5.1 Bias and correlation of hourly wind speed

Based on the 26 data sets involved in the remodeling process a general correction function was derived by a multiple linear regression model for the slope and offset parameter. This general correction function was then applied to each of the raw data sets. These data sets are considered "semi-independent" as their specific correction function was used to derived the overall mean correction function but the latter was applied for the final correction. The same argument holds for the offshore met masts. The remaining 22 onshore data sets not used for the remodeling process are considered independent.

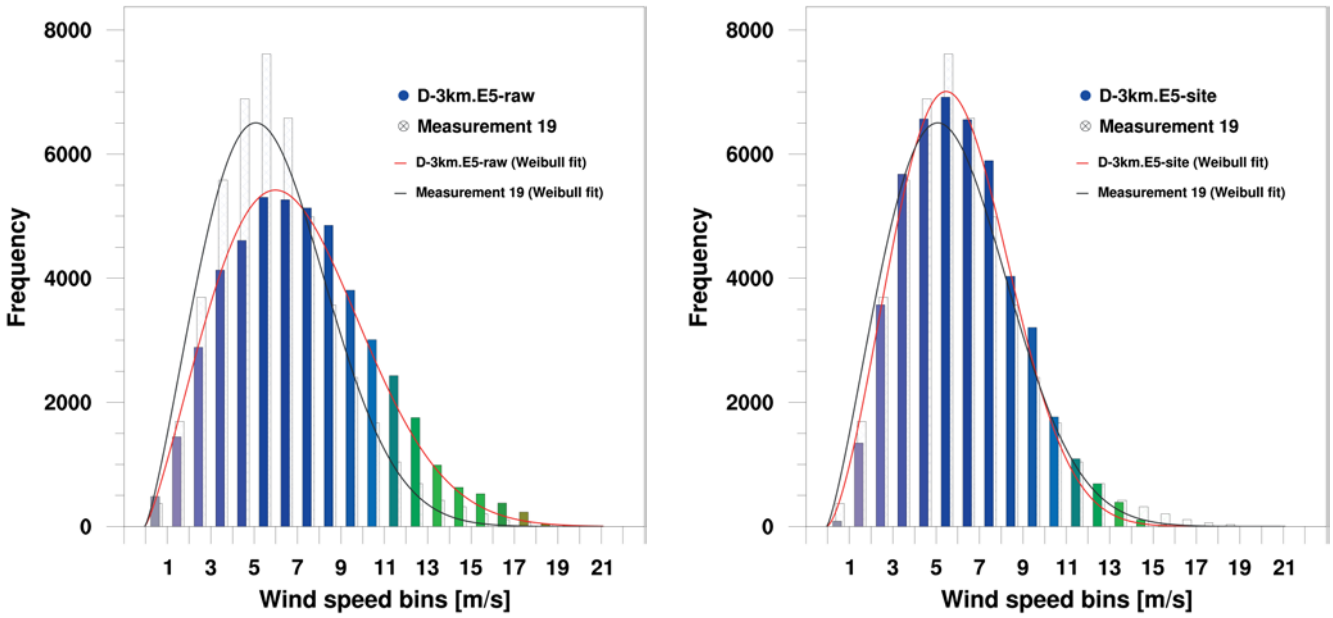

Figure 5: Exemplary wind speed frequency distribution of the raw data (left) and after the remodeling process (right) for measurement site 19. The color shifts from blue to green for higher wind speed bins.

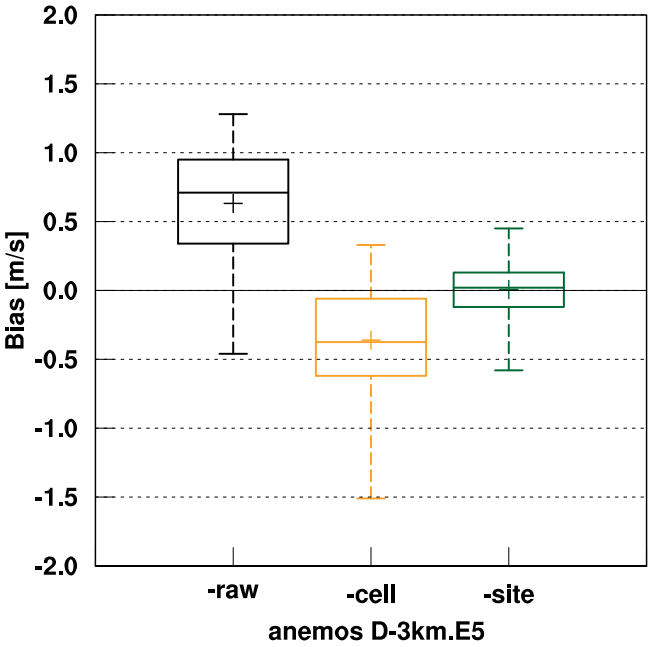

Figure 6: Three box plots showing the biases of the comparison of raw wind atlas data, remodeled data ("cell") and site-specific data ("site") for the 48 onshore measurement sites for 100 m height. The crosses mark the average of all stations (mean bias). The horizontal bars in the box indicates the median and the box borders the quartiles, respectively. Minimum and maximum are indicated by the whiskers.

As a result of the remodeling process the bias of the mean wind speed is reduced at all met masts. Before the remodeling process the model showed a positive bias (model winds were too strong) for almost all onshore met masts of up to 27 percent and a negative bias of less than 5 percent for offshore conditions. The mean bias for all data sets before and after the remodeling process is shown in Fig. 7. Obviously, the bias is low for the offshore met masts as there were only four data sets and the deviation of the respective scaling factor to the mean factor is small in any case due to the similar surface characteristics. For the onshore sites the effect of the remodeling is remarkable. Most of the onshore data show a mean bias well within the range of ±5 % with some exceptions for very complex sites (Black Forest and Swiss Alps). It seems that even with a site-specific correction mesoscale data with 3 km resolution find their limit of reasonability at those sites. An error of 5 % in mean wind speed would result in an error for the wind turbine electricity production of approximately 10 % to 15 %, depending on the wind speed frequency distribution and turbine power curve characteristics (a factor between 2 and 2.5 is a reasonable choice). From our long year consultancy experience an overall uncertainty of up to 15 % for the mean annual power production appears to be acceptable for the wind industry.

The mean bias over all measurements (Fig. 8) is close to zero for all three data sets (onshore semi-independent, onshore independent, offshore) while the standard deviation and outliers (extremes of the bias) show a wider spreading for the independent data set.

For a subset of the measurements the analysis was also performed for 60 m, 80 m, and 140 m height (Table 1). As expected, the bias and its standard deviation decrease with increasing height as the influence of a major uncertainty factor, namely the parameterization of the surface characteristic in the mesoscale model, is reduced with increasing height. The bias reduction is highest from 60 m to 80 m and reduced also for the 80 m

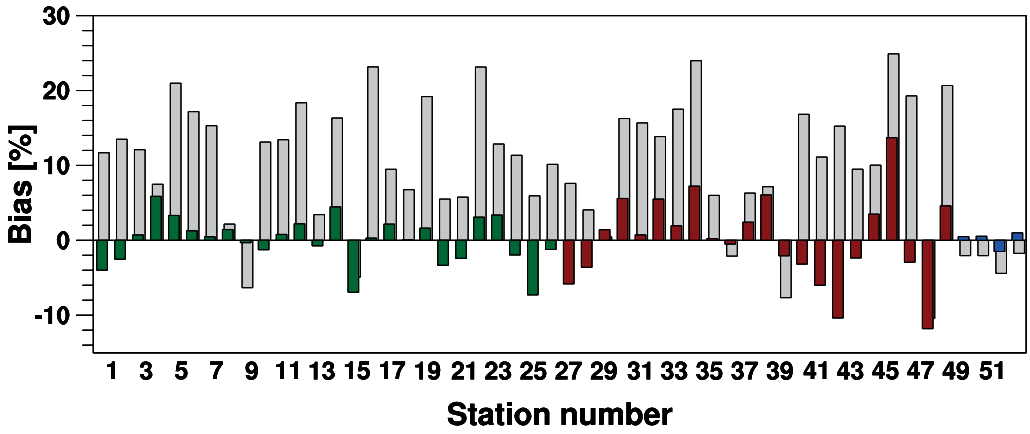

Figure 7: Bias in mean wind speed for "raw data" (grey) and "remodeled site-specific data" divided into "semi-independent" (green) and "independent" (red) onshore data and the offshore met masts (blue) for 100 m height.

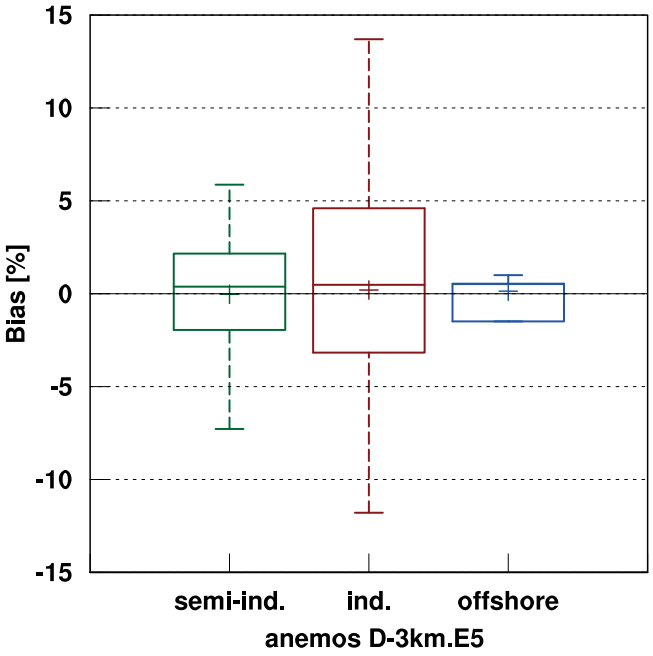

Figure 8: Mean bias in wind speed, standard deviation and extreme values for "semi-independent" (green) and "independent" (red) onshore data and the offshore met masts (blue) for 100 m height.

to 100 m step. The correlation of the hourly time series increases with height from 84.3 % at 60 m to 87.4 % at 140 m.

In order to demonstrate the quality of the remodeled mesoscale data set by a fully independent process, time series of the wind atlas were provided to an institution not linked to anemos GmbH for a given set of 66 sites (Fig. 9). The analysis was performed on the whole by the market competitor Ramboll Deutschland GmbH. Only the site coordinates were known by the anemos team. Ramboll's analyses are in remarkable agreement with the results shown before. With a mean bias of 0.4 % and a root mean square error of 4.5 % for the measurements between 85 m and 164 m height the results are

Table 1: Mean bias and correlation coefficient in wind speed for measurements at different heights after the remodeling approach.

Height [m]	No. of sites	Bias [%]	Bias [m/s]	R [%]
60	38	3.82 ± 7.18	0.15 ± 0.31	84.3 ± 4.8
80	45	0.50 ± 5.02	0.01 ± 0.26	85.9 ± 3.9
100	52	0.08 ± 4.38	0.00 ± 0.24	86.9 ± 3.6
140	17	0.10 ± 3.45	0.01 ± 0.21	87.4 ± 2.9
Ramboll 85–164	66	0.40 ± 4.5	—	87.3 ± 2.3

only slightly higher than our results as is the correlation coefficient with 87.3 %.

Poulos and Stoelinga (2020) compared mesoscale model simulations with measurements at 105 sites with 2 to 10 meteorological towers each. No detailed information about model settings and measurement heights is available but for different model resolutions the bias for wind speed was found in the range of 1.9 % for 200 m resolution to 3.6 % for 600 m resolution. This data are in line with our statement that with downscaled mesoscale model data a bias for the mean wind speed below 5 % is reasonable. This complies with the uncertainty requirements for the wind energy industry.

5.2 Correction of the annual cycle

The effect of correcting the annual cycle was also investigated for the Ramboll data set. For 39 met masts the mean monthly deviation, its standard deviation, and the extremes are shown for the raw wind atlas data (no remodeling) and the time series after the remodeling process in Fig. 10. Like our analysis (Fig. 3) the correction reduced the positive deviation in winter and the negative deviation in summer and lead to a more realistic annual cycle of the wind speed.

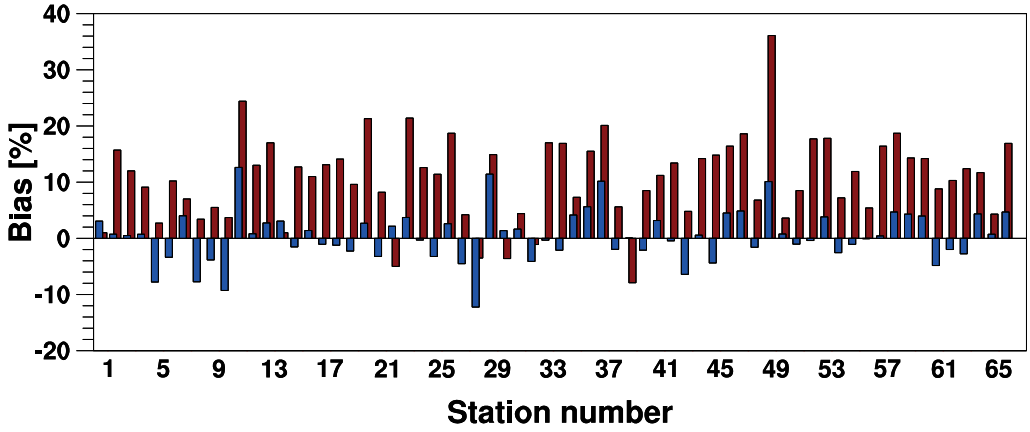

Figure 9: Bias of 66 measurements for "raw data" (red) and "remodeled site-specific data" (blue) based on Ramboll analysis.

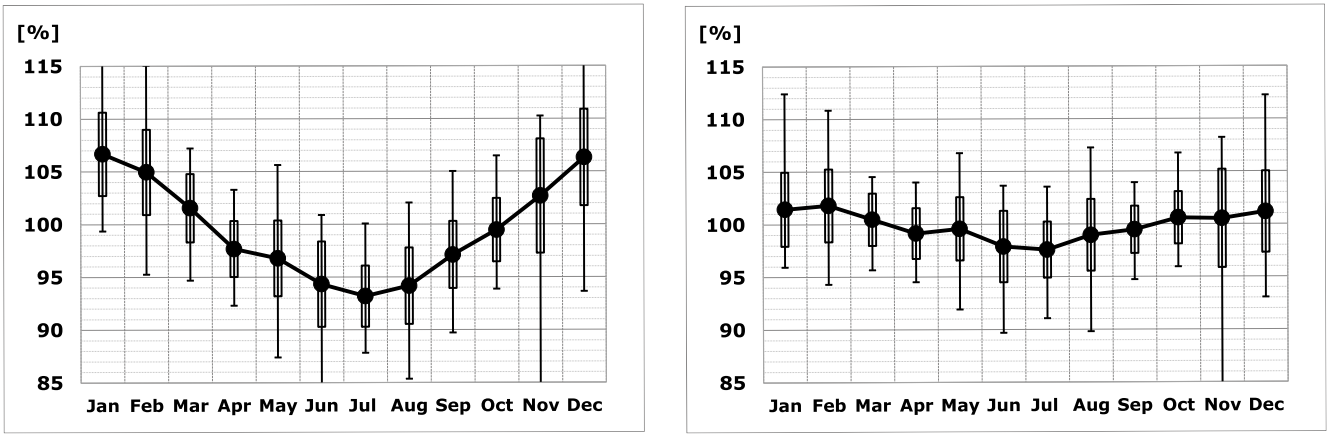

Figure 10: Monthly bias of 39 measurements for the Ramboll data, raw data (left) and corrected data (right). The boxes represent the standard deviation and the thin bars show extremes.

5.3 Frequency distribution of wind speed and direction

The wind speed frequency distribution may be approximated by a Weibull distribution with scale parameter A [m/s] and shape parameter k. The scale parameter is linked to the position of the maximum of the distribution and is slightly larger than the mean wind speed. The shape parameter k is a measure of the width of the distribution i.e. the variance of wind speed. Fig. 11a shows the absolute k values for the measurement and remodeled simulation results. Most of the k values of the 52 measurements are in a small box with a range of ±0.2. The simulated mean and 25/75 quantile are slightly shifted to higher values, but the outliers (extremes of k) are in a similar range. Fig. 11b displays the bias in k (simulation minus measurement) with a mean value of 0.06 and standard deviation of 0.1. The Weibull A parameter shows a zero biased distribution with a standard deviation of 4.1 % (Fig. 11c). The Weibull distribution commonly is considered to reasonably well represent the wind speed distribution for Northern Europe long year wind conditions.

The bias and correlation of the wind direction for the 52 measurement sites is shown in Fig. 12. The realistic representation of the wind direction is of paramount importance for the siting of wind turbines in a wind farm as it governs the wind farm wake effect. Although wind vanes are usually aligned carefully small mounting errors cannot be excluded. The overall bias in direction shows a positive mean value of 1.5° with a standard deviation of 3.0°. These deviations are covered in the uncertainty of the wind vanes. No correction was made for wind direction. The correlation reaches 95 % for more than half of the stations. An example of the wind direction distribution is given exemplary for 100 m height at site 19 (Fig. 13). The excellent agreement between simulated and observed wind direction is considered an effect of the reduced roughness influence at 100 m height and the dominating pressure gradient.

5.4 Comparison with NEWA and EMD data sets

Two other data sets from model simulations are quite similar to the one discussed so far. There is the

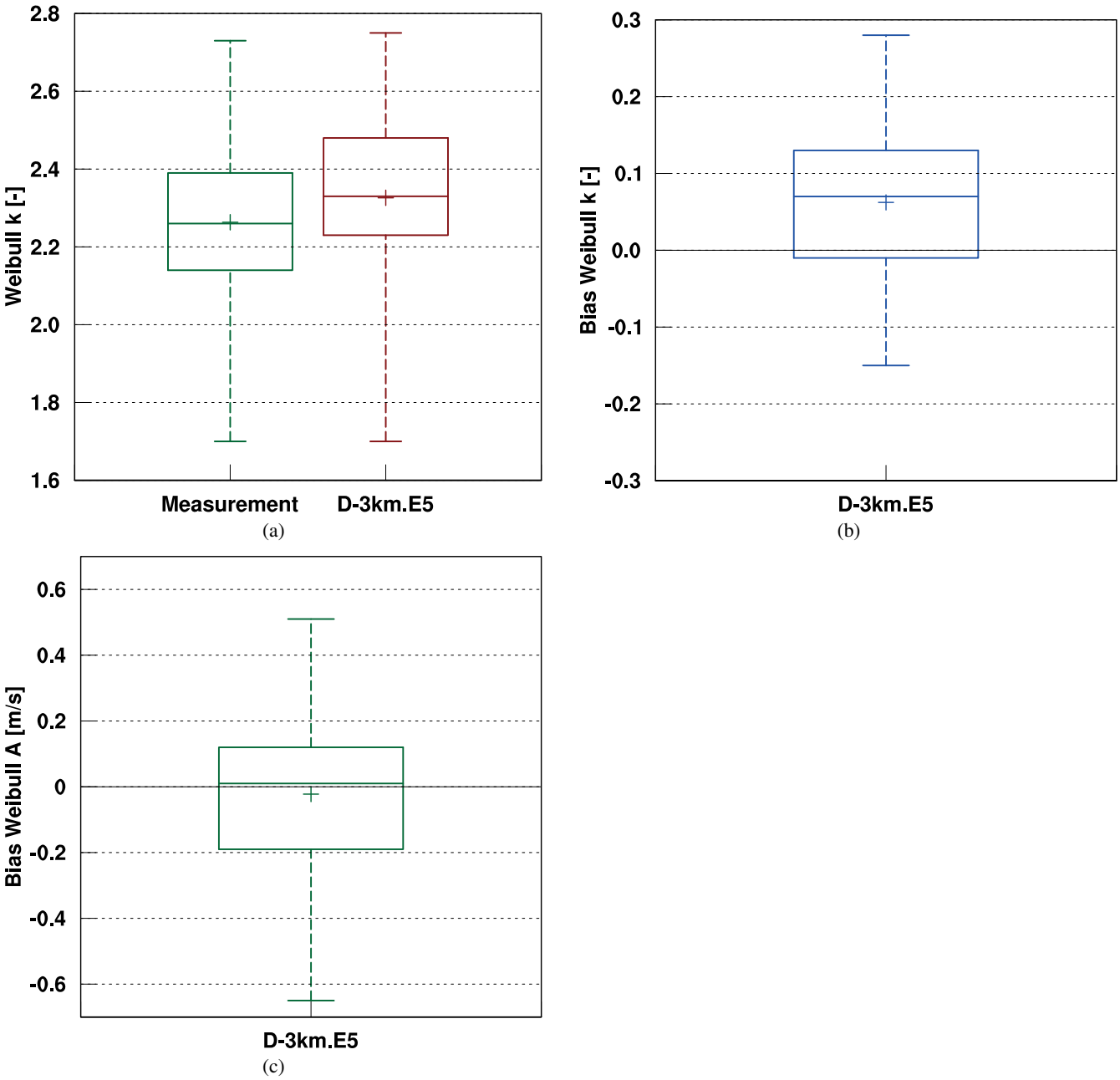

Figure 11: Consistency of the wind speed frequency distribution of 52 measurements at 100 m height represented by Weibull parameter k (a)–(b) and A (c).

New European Wind Atlas NEWA, (NEWA, 2020; Gottschall et al., 2019; Witha et al., 2019; González-Rouco et al., 2019, Dörenkämper et al., 2020) and the EMD-WRF EUROPE+ mesoscale data set (EMD, 2020a). The official wind atlas data sets have been downloaded from the respective data base and no correction has been applied by us. Differences in model version (anemos: WRF 3.7.1, NEWA: WRF 3.8.1) and set-up (anemos: 50 vertical layers, NEWA: 61), parameterization schemes (anemos: Yonsei University (YSU) planetary boundary layer scheme, NEWA: modified Mellor–Yamada–Nakanishi–Niino (MYNN) planetary boundary-layer scheme), boundary conditions (anemos: ERA5 SST with hourly assimilation, NEWA: OSTIA SST with 6-hourly assimilation), and simulation runs (anemos: multi-year simulations with 1 month spin-up, NEWA: 8 day simulations with 24 h spin-up) exist. No such information is available for the EMD-WRF data set. All three simulations, however, use the ERA5 reanalysis as forcing data, a validated version of the WRF mesoscale model and a 3 km horizontal grid resolution. Use of the data for the wind energy industry is the main purpose of all data sets. It is not our intention to discuss potential discrepancies between these data sets in terms of model configuration or simulation approach but rather highlight the effect of the remodeling process. We used those 22 wind measurements which were not part of the determination of the remodeling parameters and calcu-

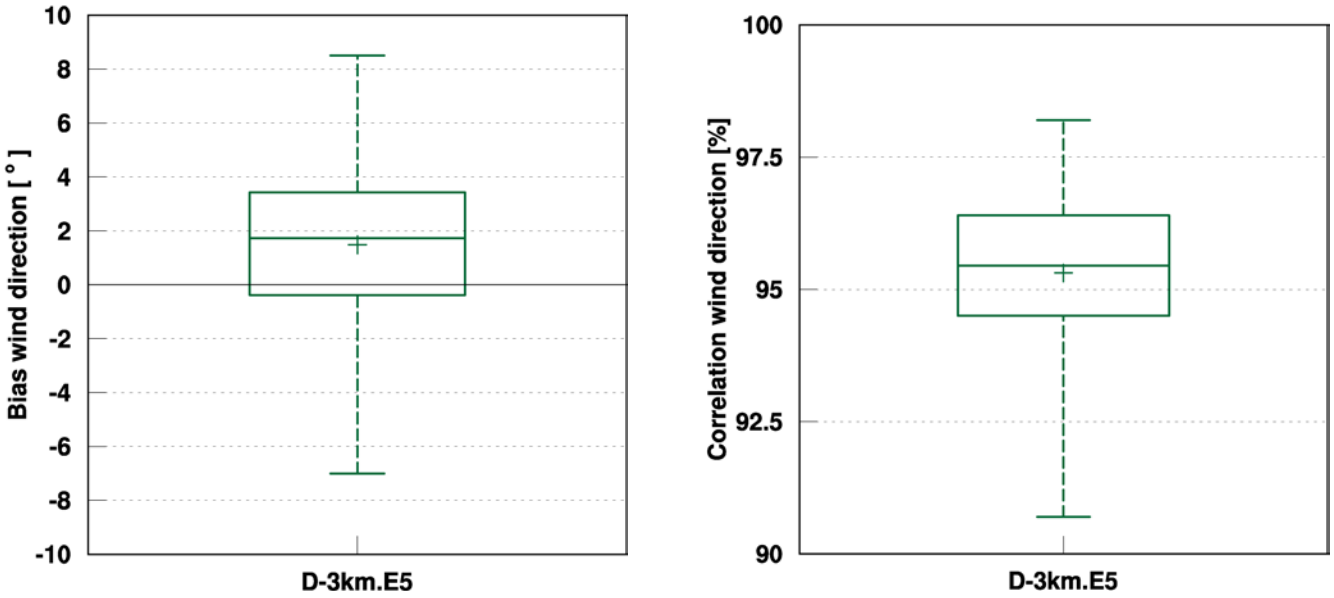

Figure 12: Consistency of the wind direction of 52 measurements at a mean height of 98 m.

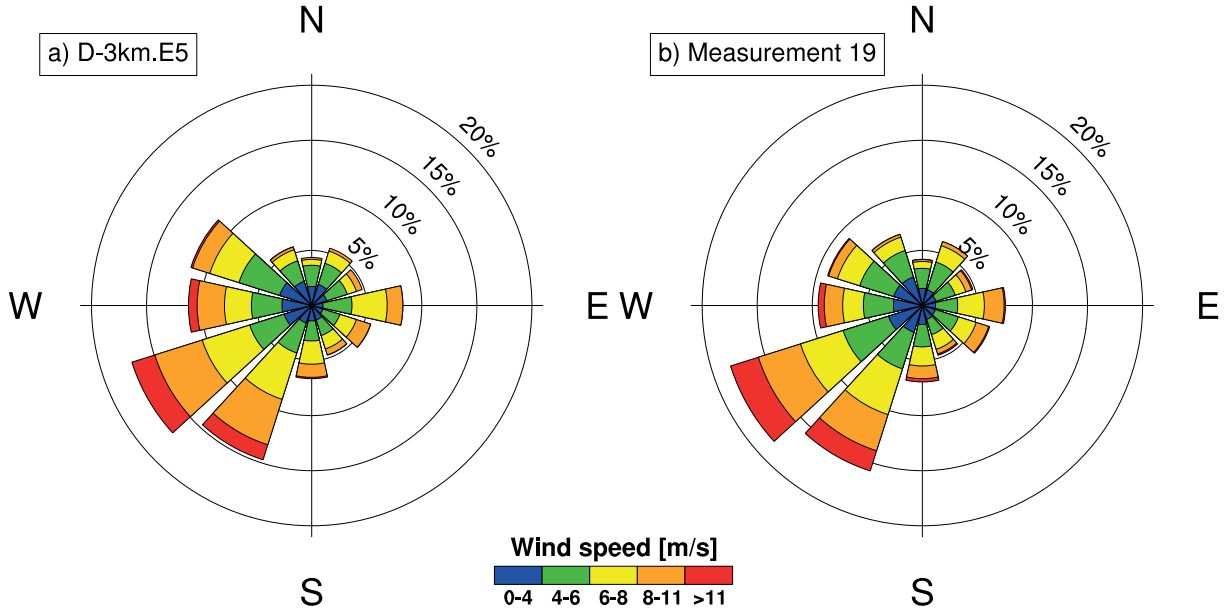

Figure 13: The wind roses simulated (left) and observed (right) at site 19 at 100 m height.

lated the overall bias and correlation for the 100 m height data from the different simulations. Figs. 14a and b show the bias and correlation in wind speed for the following data sets:

a) NEWA data

b) EMD-WRF Europe+ data

c) anemos raw data without any remodeling or adaptation process

d) anemos wind atlas after remodeling (= cell)

e) anemos wind atlas after remodeling site specific (= site).

Data sets a)–d) are is the model output on the 3 km grid while for data set e) the respective 3 km data have been itemized for the met mast site to be compared with. This process uses orography and land-use information to adapt the time series on the 3 km grid to the surface characteristics in the immediate vicinity of the met mast. The adaptation is based on findings from the remodeling process. At this point it must be emphasized that the general findings from the remodeling process using 26 met masts are applied here to an independent data set consisting of the remaining 22 measurements. With a mean coefficient of 81.2 % the correlation of hourly data is lowest for the NEWA data followed by the EMD-WRF Europe+ data with 85.2 % and 86.8 % for the three anemos data sets. Because the ERA5 re-

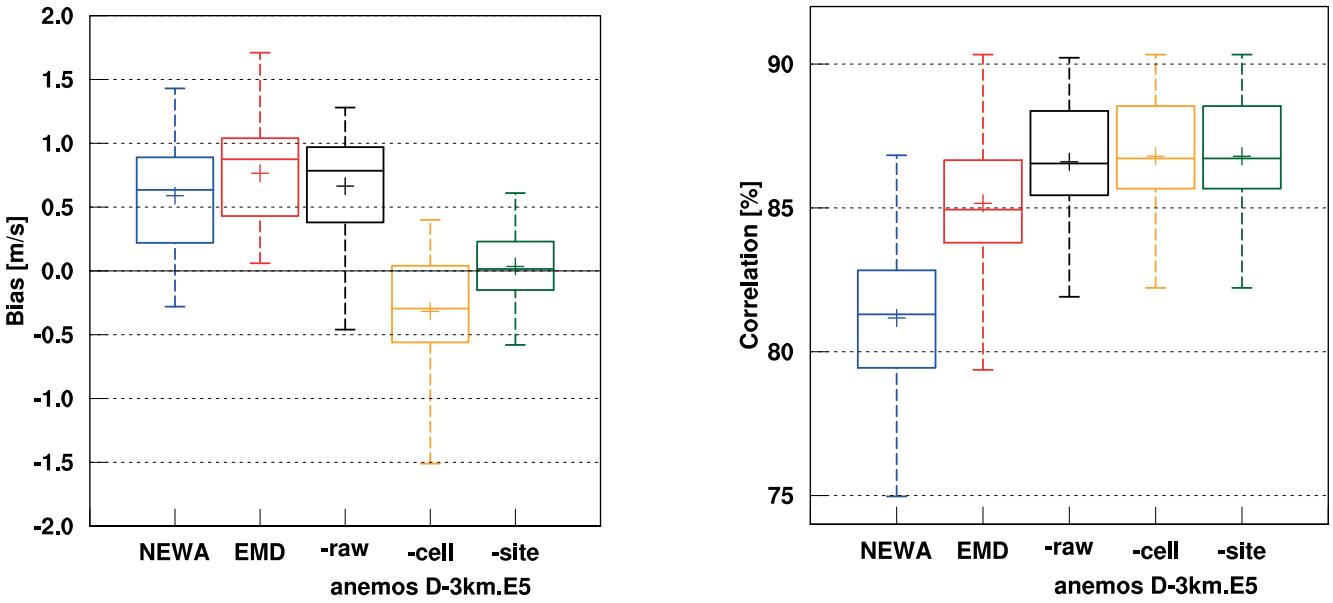

Figure 14: Boxplots of the bias (left) and correlation (right) in wind speed for 22 independent sites. Compared are three versions of the anemos wind atlas, namely the raw data (black) and the corrected data on a 3 km grid (orange) and the site specific data (green) with the NEWA (blue) and EMD-WRF Europe+ wind (red) atlas.

analysis is the forcing for all simulations the difference in the correlation might be due to various WRF model configurations or simulation realizations (e.g. nudging technique and time step, length of simulation period). In addition, the anemos and EMD-WRF EUROPE+ hourly data represent the average of 10-min instantaneous values whereas the NEWA data are based on 30-min instantaneous values. An investigation into the sensitivity of the correlation coefficient on model settings is not our intent. However, a difference of 5.6 % in the correlation seems to be rather large keeping in mind that e.g. the electricity price is dealt on the Stock Exchange half-hourly. The picture is quite different for the bias. All three raw data sets without any remodeling or adaptation have a mean bias in a similar range between +0.6 and +0.8 m/s. After remodeling the bias of the anemos wind atlas is overcompensated with a negative value of −0.3 m/s. This is explained by the fact that met masts for wind energy purposes commonly are positioned at exposed sites compared to the average height of a model grid cell. The site-specific mean wind speed corrects for this overestimation and finally shows a mean bias of 0 with an extend of 0.3 m/s for the 25 % to the 75 % quartile (50 % of the data within this box). Also, the spread of the bias is reduced compared to the non-remodeled data.

6 Conclusion and outlook

This paper is based on the idea that even small uncertainties in wind speed may result in large uncertainties for the wind potential and wind turbine power production and may imply an increased risk for investments in wind energy projects. Hence, reducing the uncertainty of wind simulations to the extent possible is of particular importance for applications in the wind energy sector.

This paper compares wind simulations and observations at 118 met masts and describes a remodeling approach to reduce the inherent difference between model output and observations. The mesoscale model WRF is used to simulate the wind conditions over Germany with a horizontal resolution of $3 \times 3\,\mathrm{km}^2$ and a temporal resolution of 10-min. The analysis, however, is made with aggregated hourly data. ERA 5 reanalysis data are used for forcing purposes.

In order to minimize the inherent difference between simulations and observations a remodeling approach is applied which corrects simulated wind speed time series taking into account differences in surface characteristics (height and roughness variations) between model grid cell and observation site. The remodeling process comprises 4 main steps followed by a site-specific adaptation:

a) Correction of the annual cycle.

b) Correction for height difference between model grid cell and measurement point. The speed-up factors are deduced from CFD model simulations.

c) Derivation of regression parameter (slope and offset) between simulated and observed wind speed for 8 direction sectors at 26 measurement sites. Multiple linear regression analysis separately for slope and offset to derive a global parameter set. Remodeling the mesoscale wind speed time series resulting in a reconditioned wind atlas.

d) Site-specific adaptation of mesoscale wind speed time series.

The "raw" wind atlas data (before step a), the reconditioned wind atlas data (after step c) and the site-specific data (after step d) were compared to observations at 100 m height. The "raw" data showed a positive bias of up to 27 % for the mean wind speed onshore and a negative bias of less than 5 % for the offshore towers. The remodeled data (after step d) showed a mean negative bias for onshore sites. This is explained by the fact that measurements for the wind industry tend to be performed at exposed sites. This effect was corrected for with the site-specific adaptation.

Accounting for all 118 met masts and a height range between 80 m and 160 m the mean bias in wind speed is roughly within a range of 0.08 % and 0.50 % with a standard deviation below 5 %. A 5 % uncertainty in wind speed is in the range expected today for financial considerations in the wind energy industry.

The wind speed frequency distribution expressed by Weibull parameter showed a bias close to zero with a standard deviation of roughly 4 % for the scale parameter A and a mean bias less than 0.1 for the form parameter *k*. The small mean bias of 1.5 deg in wind direction is not corrected for as it might be in the range of the mounting uncertainty.

Comparison of the NEWA and EMD-WRF Europe+ wind atlas data with observations showed a mean bias between +0.6 m/s and +0.8 m/s similar to our "raw" data. The remodeling and site-specific adaptation process significantly reduced the mean bias to 0.03 m/s with a standard deviation of 0.27 m/s.

A method was presented to minimize the discrepancy between wind simulations and measurements by a remodeling process and a site-specific adaptation. The resulting uncertainty is in a the range which is acceptable by the wind industry even for financial considerations. Such data sets will form an essential contribution to the wind farm development process. The anemos wind atlas data sets are commercially available via the awis (anemos wind information system, awis.anemos.de) online tool.

Acknowledgements

This paper is based on data provided by wind farm owners and developers. The study was partly supported by N-Bank Niedersachsen and the Federal Ministry for the Environment, Nature Conservation and Nuclear Safety represented by the German Environment Agency of the Federal Republic Germany. The final form of this paper benefitted from the helpful comments and suggestions of the two anonymous reviewers.

References

Badger, J., H. Frank, A.N. Hahmann, G. Giebel, 2014: Wind-climate estimation based on mesoscale and microscale modeling: statistical-dynamical downscaling for wind energy applications. – J. Appl. Meteor. Climatol. **53**, 8, 1901–1919, DOI: 10.1175/JAMC-D-13-0147.1.

Carvalho, D., A. Rocha, M. Gómez-Gesteira, C. Silva-Santos, 2014: WRF wind simulation and wind energy production estimates forced by different reanalyses: Comparison with observed data for Portugal. – Appl. Energy **117**, 116–126.

C3S – Copernicus Climate Change Service, 2017: ERA5: Fifth generation of ECMWF atmospheric reanalyses of the global climate. – Copernicus Climate Change Service Climate Data Store (CDS), date of access. https://cds.climate.copernicus.eu/cdsapp#!/home.

Deppe, A.J., W.A. Gallus Jr., E.S. Takle, 2013: A WRF ensemble for improved wind speed forecasts at turbine height. – Wea. Forecast. **28**, 212–228, DOI:10.1175/WAF-D-11-00112.1.

Dörenkämper, M., B.T. Olsen, B. Witha, A.N. Hahmann, N.N. Davis, J. Barcons, Y. Ezber, E. García-Bustamante, J.F. González-Rouco, J. Navarro, M. Sastre-Marugán, T. Sile, W. Trei, M. Žagar, J. Badger, J. Gottschall, J.S. Rodrigo, J. Mann, 2020: The Making of the New European Wind Atlas – Part 2: Production and evaluation. – Geosci. Model Dev. **13**, 5079–5102.

EMD, 2020a: EMD-WRF Europe+ MesoScale Data Set. – https://www.emd.dk/data-services/mesoscale-time-series/pre-run-time-series/emd-wrf-europe-mesoscale-data-set/.

EMD, 2020b: windpro Technical Note: Validation of EMD-WRF EUROPE+ (ERA5) mesoscale dataset, EMD International A/S. – http://help.emd.dk/knowledgebase/content/Technotes/TechnicalNote7_EMDWRF_EUROPE_Validation.pdf.

Farr, T.G., P.A. Rosen, E. Carop, R. Crippen, R. Duren, S. Hensley, M. Kobrick, M. Paller, E. Rodriguez, L. Roth, D. Seal, S. Shaffer, J. Shimada, J. Umland, M. Werner, M. Oskin, D. Burbank, D. Alsdorf, 2007: The Shuttle Radar Topography Mission. – Rev. Geophys. **45**, 2, DOI:10.1029/2005RG000183.;

Fernández-Gonzales, S., M.L. Martin, E. Garcia-Ortega, A. Merino, J. Lorenzana, J.L. Sanchez, F. Valero, J.S. Rodrigo, 2018: Sensitivity analysis of the WRF model: Wind-resource assessment for complex terrain, J. Appl. Climatol. **57**, 3, 733–753, DOI:10.1175/JAMC-D-17-0121.1

Giannakopoulou, E.-M., R. Nhili, 2014: WRF Model Methodology for Offshore Wind Energy Applications. – Adv. Meteor., published online, 319819, DOI:10.1155/2014/319819.

González-Rouco, J.F., E. Garcia-Bustamante, A.N. Hahmann, I. Karagili, J. Navarro, B.T. Olsen, T. Sile, B. Witha, 2019: NEWA. – Report on uncertainty quantification. – https://zenodo.org/record/3382572#.XnHzAHdFxPY.

Gottschall, J., M. Dörenkämper, B. Lange, P. Kühn, D. Callies, B. Witha, G. Steinfeld, S. Voss M. Kühn, D. Heinemann, 2019: NEWA – New European Wind Atlas Joint Programme. – Final report, personal communication.

Hahmann, A.N., T. Sile, B. Witha, N.N. Davis, M. Dörenkämper, Y. Ezber, E. García-Bustamante, J.F. González-Rouco, J. Navarro, B.T. Olsen, S. Söderberg, 2020: The Making of the New European Wind Atlas, Part 1: Model Sensitivity. – Geosci Model Dev. **13**, 5053–5078, 10.5194/gmd-13-5053-2020.

Howard, T., P. Clark, 2007: Correction and downscaling of NWP wind speed forecasts. – Meteor. Appl. **14**, 105–116, DOI:10.1002/met.12.

Hu, X-M., J.W. Nielsen-Gammon, F. Zhang, 2010: Evaluation of Three Planetary Boundary Layer Schemes in the WRF Model. – J. Appl. Meteor. Climatol. **49**, 1831–1843, DOI: 10.1175/2010JAMC2432.1.

Hu, X-M., P.M. Klein, M. Xue, 2013: Evaluation of the updated YSU planetary boundary layer scheme within WRF for wind

resource and air quality assessments – J. Geophy. Res.: Atmos., **118**, 10490–10505, DOI:10.1002/10.1002/jgrd.50823.

IEC, 2017: International Electrotechnical Commission IEC 61400-12-1:2017, Wind energy generation systems – Part 12-1: Power performance measurements of electricity producing wind turbines. – International Electrotechnical Commission (IEC).

Keil, M., M. Bock, T. Esch, A. Metz, S. Nieland, A. Pfitzner, 2010: CORINE Land Cover Aktualisierung 2006 für Deutschland. Abschlussbericht zu den F+E Vorhaben UBA FKZ 3707 12 200 und FKZ 3708 12 20. – Deutsches Zentrum für Luft- und Raumfahrt e. V., Deutsches Fernerkundungsdatenzentrum Oberpfaffenhofen, Januar 2010.

Lindenberg, J., H.-T. Mengelkamp, G. Rosenhagen, 2012: Representativeness of near surface wind measurements from coastal stations at the German Bight. – Meteorol. Z. **21**, 1, 99–106.

Mengelkamp, H.-T., 1999: Wind climate simulation over complex terrain and wind turbine energy output estimation. – Theor. Appl. Climatol. **63**, 129–139, DOI:10.1007/s007040050098.

Mengelkamp, H.-T., H. Kapitza, U. Pflüger, 1997: Statistical-dynamical downscaling of wind climatologies. – J. Wind Eng. Ind. Aerodyn. **67–68**, 449–457.

METEODYN WT, 2015: Technical note-meteodyn WT. – Technical report, https://meteodyn.com/.

NEWA, 2020: About the New European Wind Atlas, https://map.neweuropeanwindatlas.eu/about.

Olsen, B.T., A.N. Hahmann, A.M. Sempreviva, J. Badger, H.E. Jørgensen, 2017: An intercomparison of mesoscale models at simple sites for wind energy applications. – eWind Energ. Sci. **2**, 211–228, www.wind-energ-sci.net/2/211/2017/ DOI:10.5194/wes-2-211-2017.

Petersen, E.L., I. Troen, S. Frandsen, K. Hedegaard, 1981: Danish Windatlas: A rational method for wind energy siting, Risø-R-428. – Risø National Laboratory, Denmark, 229 pp, ISSN 0106-2840.

Poulos, G.S., M. Stoelinga, 2020: Mesoscale and Microscale Modelling for Wind Energy Applications. – Windtech International. **16**, 6–8.

Serban, A., L.S. Paraschiv, S. Paraschiv, 2020: Assessment of wind energy potential based on Weibull and Rayleigh distribution models. – Science Direct, Energy Reports **6**, Suppl. 6, 250–2676, DOI:10.1016/j.egyr.2020.08.048.

Skamarock, W.C., J.B. Klemp, J. Dudhia, D.O. Gill, D.M. Barker, M.G. Duda, X.-Y. Huang, W. Wang, J.G. Powers, 2008: A description of the advanced research WRF Version 3. – NCAR Technical Note NCAR/TN-475+STR, June 2008.

Siuta, D., G. West, R. Stull, 2017: WRF hub-height wind forecast sensitivity to PBL scheme, grid length, and initial condition choice in complex terrain. – Wea. Forecast. **32**, 493–509, DOI:10.1175/WAF-D-16-0120.1.

Staffell, I., S. Pfenninger, 2016: Using bias-corrected reanalysis to simulate current and future wind power output. – Energy **114**, 1224–1239, DOI:10.1016/j.energy.2016.08.068.

Thøgersen, M.L., M. Motta, T. Sørensen, P. Nielsen, 2007: Measure-Correlate-Predict Methods: Case Studies and Software Implementation. – presented at European Wind Energy Conference, Milan.

Weiter, A., M. Schneider, D. Peltret, H.-T. Mengelkamp, 2019: Electricity production by wind turbines as a means for the verification of wind simulations. – Meteorol. Z. **28**, 1, 69–77, DOI:10.1127/metz/2019/0924.

Wieringa, J. 1980: Representativeness of wind observations at airports. – Bull. Amer. Meteor. Soc. **61**, 962–971.

Wieringa, J., 1996: Does Representative Wind Information Exist? – J. Wind Eng. Ind. Aerodyn. **65**, 1–12.

Witha, B., A.N. Hahmann, T. Sile, M. Dörenkämper, Y. Ezber, E. Garcia-Bustamante, J. Fidel Gonzalez-Rouco, G. Leroy, J. Navarro, 2019: NEWA, Report on WRF model sensitivity studies and specifications for the mesoscale wind atlas production runs. – https://zenodo.org/record/2682604#.XnH3GohKiHt.

WRF, 2017: User's Guides for the Advanced Research WRF (ARW) Modeling System, Version 3. – WRF user page, http://www2.mmm.ucar.edu/wrf/users/docs/user_guide_V3/contents.html.

Yang, Q., L.K. Berg, M. Pekour, J.D. Fast, R.K. Newsom, M. Stoelinga, C. Finley, 2013: Evaluation of WRF-Predicted Near-Hub-Height Winds and Ramp Events over a Pacific Northwest Site with Complex Terrain. – J. Appl. Meteor. Climatol. **52**, 8, 1753–1763, DOI:10.1175/JAMC-D-12-0267.1.